



**HAL**  
open science

# Performance loss of proton exchange membrane fuel cell due to hydrophobicity loss in gas diffusion layer: Analysis by multiscale approach combining pore network and performance modelling

Joel Pauchet, Marc Prat, Pascal Schott, Srijith Pulloor Kuttanikkad

## ► To cite this version:

Joel Pauchet, Marc Prat, Pascal Schott, Srijith Pulloor Kuttanikkad. Performance loss of proton exchange membrane fuel cell due to hydrophobicity loss in gas diffusion layer: Analysis by multiscale approach combining pore network and performance modelling. *International Journal of Hydrogen Energy*, 2012, vol. 37, pp. 1628-1641. 10.1016/j.ijhydene.2011.09.127 . hal-00925579

**HAL Id: hal-00925579**

**<https://hal.science/hal-00925579>**

Submitted on 8 Jan 2014

**HAL** is a multi-disciplinary open access archive for the deposit and dissemination of scientific research documents, whether they are published or not. The documents may come from teaching and research institutions in France or abroad, or from public or private research centers.

L'archive ouverte pluridisciplinaire **HAL**, est destinée au dépôt et à la diffusion de documents scientifiques de niveau recherche, publiés ou non, émanant des établissements d'enseignement et de recherche français ou étrangers, des laboratoires publics ou privés.



## Open Archive TOULOUSE Archive Ouverte (OATAO)

OATAO is an open access repository that collects the work of Toulouse researchers and makes it freely available over the web where possible.

This is an author-deposited version published in : <http://oatao.univ-toulouse.fr/>  
Eprints ID : 10489

**To link to this article** : doi:10.1016/j.ijhydene.2011.09.127  
URL : <http://dx.doi.org/10.1016/j.ijhydene.2011.09.127>

<p><b>To cite this version</b> : Pauchet, Joel and Prat, Marc and Schott, Pascal and Pulloor Kuttanikkad, Srijith Performance loss of proton exchange membrane fuel cell due to hydrophobicity loss in gas diffusion layer: Analysis by multiscale approach combining pore network and performance modelling. (2012) International Journal of Hydrogen Energy, vol. 37 (n° 2). pp. 1628-1641. ISSN 0360-3199</p>
--

Any correspondence concerning this service should be sent to the repository administrator: [staff-oatao@listes-diff.inp-toulouse.fr](mailto:staff-oatao@listes-diff.inp-toulouse.fr)

# Performance loss of proton exchange membrane fuel cell due to hydrophobicity loss in gas diffusion layer: Analysis by multiscale approach combining pore network and performance modelling

Joël Pauchet<sup>a,\*</sup>, M. Prat<sup>b,c</sup>, P. Schott<sup>a</sup>, S. Pulloor Kuttanikkad<sup>d</sup>

<sup>a</sup>CEA, LITEN, LCPEM, Laboratory of Fuel Cell Components, Electrolysers and Modeling, 17 rue des Martyrs, 38054 Grenoble, France

<sup>b</sup>Université de Toulouse, INPT, UPS, IMFT, Avenue Camille Soula 31400, Toulouse, France

<sup>c</sup>CNRS, IMFT 31400, Toulouse, France

<sup>d</sup>Shell Global Solutions International, The Netherlands

## ABSTRACT

Loss of hydrophobicity in the gas diffusion layers (GDL) is sometimes suggested as a potential mechanism to explain in part the performance loss of PEMFC. The present study proposes a numerical methodology to analyse this effect by combining pore network modelling (PNM) and performance modelling (PM): the PNM/PM approach. PNM allows simulating the decrease of through-plane gas diffusion coefficient in the GDL as a function of the hydrophobicity loss, which is taken into account through the increase in the fraction of hydrophilic pores in GDL. Then PM based on Darcy equations allows simulating performance loss of PEMFC as a function of gas diffusion decay. This coupling shows that the loss of hydrophobic treatment increases flooding, decreases performance, and increases current density heterogeneities between inlet and outlet of the cell. Interestingly, this degradation is found to be highly non-linear, mainly because of the non-linear influence of the fraction of hydrophilic pores on gas diffusion (this is due to the existence of a percolation threshold associated with the hydrophilic pore sub-network) as well as the non-linear behaviour of electrochemistry with gas diffusion. This study also shows that the loss of hydrophobicity in a GDL is a very suitable candidate to explain performance loss rates that are classically observed during long-term tests. The proposed methodology may also help linking other local properties of components to fuel cell global performance.

Copyright

## Keywords:

PEM fuel cell  
Gas diffusion layer  
Two-phase flow  
Pore network model  
Degradation  
Multiscale coupling

## 1. Introduction

Proton Exchange membrane fuel cells (PEMFCs) are one of the most promising solutions as an alternative to combustion engine with no pollution emission. Nevertheless, before their

industrialisation for automotive application, some bottlenecks are to be solved to reduce their cost and to increase their durability [1,2]. Numerous degradation mechanisms have already been observed or are suggested to explain performance loss of PEMFC (mechanical deformation, chemical

\* Corresponding author. Tel.: +33 (0)4 38 78 52 96.

E-mail address: joel.pauchet@cea.fr (J. Pauchet).

Nomenclature	
A	cross-section, m <sup>2</sup>
a	thermodynamic activity, –
C	concentration, mol m <sup>-3</sup>
D	diffusion coefficient, m <sup>2</sup> s <sup>-1</sup>
D <sub>eff</sub>	effective diffusion coefficient, m <sup>2</sup> s <sup>-1</sup>
d <sub>p</sub>	pore diameter, m
d <sub>t</sub>	throat diameter, m
E	equilibrium potential, V
EW	equivalent weight of Nafion, g/eq
e	thickness, m
F	Faraday constant, 96,485 C mol <sup>-1</sup>
f	fraction of hydrophilic pores
f <sub>c</sub>	hydrophilic sub-network percolation threshold
i	current density, A m <sup>-2</sup>
J	molar flux, mol s <sup>-1</sup>
K <sub>p</sub>	pressure drop coefficient, Pa m <sup>-4</sup> s
L	length, m
M	molar mass, kg mol <sup>-1</sup>
N	molar flux density, mol m <sup>-2</sup> s <sup>-1</sup>
n <sub>eo</sub>	electro-osmotic drag coefficient, –
P	pressure, Pa
Q	flow rate, m <sup>3</sup> s <sup>-1</sup>
R	resistivity, ohm m <sup>2</sup>
S	saturation, –
S <sub>BT</sub>	saturation at breakthrough, –
T	temperature, K
t	time, h
U	voltage, V
X	molar fraction, –
z	coordinate along the channel length, m
<i>Greek</i>	
α	parameter of the electrochemical law
β	parameter of the electrochemical law
δ	parameter of the Weibull law used in PNM
ρ	density, kg m <sup>-3</sup>
η	Overpotential, V
λ	membrane water content, –
λ'	parameter of the Weibull law used in PNM
γ	parameter of the Weibull law used in PNM
σ	conductivity, S m <sup>-1</sup>
θ	contact angle, °
<i>Subscripts</i>	
act	activation
dry	related to dry porous medium
eff	effective
eo	electro-osmotic
g	gas
inlet	inlet of the cell
m	membrane
max	maximum
min	minimum
outlet	outlet of the cell
n	nitrogen
rev	reversible
sat	saturation
v	vapour
x	oxygen (at the cathode) or hydrogen (at the anode)
<i>Acronyms</i>	
CL	catalyst layer
DMFC	direct methanol fuel cell
GDL	gas diffusion layer
IP	invasion percolation
LBM	lattice Boltzmann modelling
MC	Monte-Carlo
MEA	membrane-electrodes assembly
MPL	microporous layer
PEMFC	proton exchange membrane fuel cell
PM	performance modelling
PNM	pore network modelling
PTFE	polytetrafluoroethylene
REV	representative elementary volume

modification, dissolution, thermal stress, etc). They concern each component of the cell (membrane, active layer, gas diffusion layer, bipolar plates) as well as each material (catalyst, electrolyte, carbon fibres, carbon grains, etc). A complete review of these mechanisms is beyond the scope of this paper but more details can be found in [1–3] for instance. Despite the different studies, most of these mechanisms are not sufficiently understood [2]. Evaluating the relative influence of each of them on the global performance loss is very difficult for the time being. Gas diffusion layers (GDLs) are already known as playing a crucial role on water management (see for instance [4]) and the significance of GDL contribution to degradation mechanisms is more and more suggested [1,2]. Some experimental results even show that degradation of hydrophobic treatment (including the one of GDL) can induce a performance loss two times higher than catalyst dissolution and agglomeration in the active layer [5]. This clearly shows that the degradation of GDL, although less documented than the one of active layer [2], must be taken into account to evaluate global performance loss.

The main mechanisms suggested for explaining degradation of GDL are oxidation of the carbon fibres and loss of the hydrophobic treatment [3]. After degradation, some properties of the GDL are modified. Tian [6] states that the size of the micropores of the cathode backing is reduced whereas Borup [3] states that the volume of large pores has decreased but one of the micropores has increased. Nevertheless, due to different experimental and tightening conditions, the comparison between these two results is difficult. Another major modification refers to the change of GDL hydrophobic behaviour before and after ageing. Even if an increase of hydrophobic behaviour has been reported in some cases [6], it is commonly accepted that ageing induces a loss of hydrophobic behaviour and consequently an increase of hydrophilic behaviour [1–3,5,7] and references therein. These modifications due to ageing can be different on the microporous layer (MPL) and on the backing [6], as well as on the anode side and on the cathode side [5].

It should also be pointed out that wettability is often characterised by the measurement of a “global” contact angle

on the surface of the GDL with droplets much larger than the pore size of the medium. It is therefore questionable to consider these measurements as really representative of the wettability of GDL fibrous matrix since the GDL external surface is not flat but porous. Local measurements, for instance on the pore walls, would be of major interest [1] but are not available for the moment [3]. In the absence of a better characterisation, we therefore consider that the comparison of these “global” surface contact angles is up-to-date a good way to compare wettability before and after ageing. As suggested in [1,8–10] we also consider the GDL as a mixed-wet porous medium in which some hydrophilic zones (with a contact angle  $\theta_{\text{carbone}} \sim 80^\circ$  corresponding to carbon fibres) are mixed with some hydrophobic ones (with a contact angle  $\theta_{\text{PTFE}} \sim 115^\circ$  corresponding to the coating of carbon fibres by fluoropolymer, [9]). The increase in the fraction of hydrophilic zones is assumed to be a consistent way to describe the loss of hydrophobicity. For more discussion about these hypotheses, the reader can refer to for instance [10].

As stated above, the understanding of degradation mechanisms in PEMFC requires more effort but there is also a global lack of understanding concerning the reasons why degradation of each individual component induces performance loss [2]. It is commonly suggested that the GDL loss of hydrophobicity increases the flooding and then decreases the performance [1–3] but up-to-date, no real analysis allows discussing this [2] as no approach allows linking explicitly and correctly hydrophobicity loss of GDL to performance loss of PEMFC.

To fill this gap, we propose a new modelling approach, combining performance modelling (PM) at the scale of the cell and pore network modelling (PNM) at the scale of a component (in our case the GDL on the cathode side as well as on the anode side). The approach is therefore called the PNM/PM approach.

Current PM, e.g. for instance [11–14], are based on macro-homogeneous approach in which transfers are modelled using transfer coefficients such as effective permeability, diffusion, capillary pressure, etc which are dependent on the material, on its local properties (wettability, pore sizes, etc) and also on its liquid saturation level. Unfortunately, due to experimental difficulties, most of these coefficients remain globally unknown for GDL and the scarce results [15–17] do not explain how these coefficients will be modified as a function of ageing. An additional aspect is that the relationships used in macro-homogeneous PM are based on the classical phenomenological relations, such as Darcy’s law for example, which is questionable in the case of GDL for several reasons. When the wettability is mixed, it is not easy to predict the impact of local (i.e. at the scale of microstructure) wettability changes directly at the Darcy’s scale. Scale separation between thickness of GDL and pore sizes is not sufficient and transfer coefficients depend on the thickness [18]. Water invasion regime is a function of wettability and as discussed in [19] it is not correct to use the same capillary pressure description (the so-called Leverett function) as for a purely hydrophobic system when the wettability is sufficiently modified due to the loss of hydrophobicity.

All this suggests that care should be exercised when PM are used to analyse the effect of degradation of GDL due to hydrophobicity loss on performance of PEMFC.

By contrast, PNM, see for example the review [20], are well suited to analyse fluid transfers in GDL as a function of its properties at pore scale. PNM, even when the GDL is represented by a simplified structure such as a cubic network [9,10,18], have yielded numerous interesting results not only on two-phase regime and liquid pattern inside the GDL but also on effective transfer coefficients. They allowed for instance analysing the effect of a change in wettability when the wettability is spatially uniform [19]. as well as the effect of changes in the local wettability properties in a network of mixed wettability on gas diffusion properties [10]. In the model considered in [10], a pore is either hydrophilic ( $\theta = 80^\circ$ ) or hydrophobic ( $\theta = 115^\circ$ ). The fraction of hydrophilic pores in the network can be varied and is randomly distributed within the network (hydrophilic pores correspond to local zones of GDL where the fibre surface is not covered by PTFE). The results reported in [10] show that the through-plane gas diffusion coefficient decreases as the number of hydrophilic pores in the GDL increases, due to blockage of pores by liquid water. This simple model of random distribution of hydrophilic pores suggests also the existence of a percolation threshold. When the fraction of hydrophilic pores is below this threshold, hydrophobicity loss has a small effect on gas diffusion whereas gas diffusion drastically decreases as hydrophobicity decreases above the threshold. Classical relationships for modelling gas diffusion, generally imported from studies considering porous media quite different from a GDL, are also shown to overestimate gas diffusion compared to PNM simulations [9,10].

It should be pointed out that other approaches such as Lattice Boltzmann Modelling (LBM) [21] or Monte-Carlo (MC) [22] were also developed to study two-phase flow in GDL at pore scale. Seidenberger et al. for instance [22] concludes that water content in GDL increases as hydrophobic surface of the pore decreases with the existence of a critical value above which large liquid clusters appear. This result is, at pore scale, somewhat analogous to the effect of the hydrophilic pore percolation threshold at the scale of the complete GDL [10]. However, LBM or MC implies using several grid points per pore size in each direction of space. By contrast, a pore is represented by only one grid point in PNM. As a result, computation times of LBM and MC are much higher compared to PNM. PNM thus appears as an excellent compromise between accuracy and computational efficiency compared to LBM or MC.

Nevertheless, PNM involves three-dimensional computations, which are relatively computer time demanding. PNM are therefore not adapted to the direct simulation of PEMFC performances. As mentioned before, the main idea of the present article is therefore to combine the advantages of both PNM and PM approaches to analyse the impact of the change in hydrophobicity on performances.

First link between GDL water invasion and performance was proposed by Gostick et al. [9]. This work aimed at analysing the link between mass transfer properties of GDL and the limiting current of a PEMFC, assuming that mass transfer limitation was only due to GDL. The results clearly show that liquid water invasion in the GDL has a great influence on the performance of PEMFC, at least on the limiting current which drastically decreases due to mass transfers resistances in the GDL. However, the pore network considered in [9] was 100%

hydrophobic with constant hydrophobicity ( $\theta=115^\circ$ ) and the approach did not allow calculating the complete performance of a PEMFC. By contrast, a mixed wettability network is considered in the present article and a new approach, the PNM/PM approach, is developed to predict the PEMFC performances.

In summary, the present paper has two main objectives: (i) introducing the PNM/PM approach and (ii) contributing analysing the link between loss of local wettability in GDL and loss of performance of PEMFC thanks to the PNM/PM approach.

The paper is organised as follows. Section 2 describes the methodology, i.e. how the pore network and performance models can be combined to analyse the influence of GDL structural properties on PEMFC performances. Section 3 explains how the loss of hydrophobicity in the GDL induces the decrease of GDL gas diffusion properties and then the degradation of performance of PEMFC. A discussion is then proposed to link hydrophobicity loss rate to experimental performance degradation rate. Then some concluding remarks are offered in Section 4. The paper ends with an Appendix where the equations of PM are reported.

## 2. The multiscale pore network/performance model approach to link micro-scale degradation of GDL to performance degradation

### 2.1. Motivation, overview and hypothesis

As already described in Section 1, fluid transfer coefficients in GDLs are generally poorly known and classical (Darcy's scale) models of two-phase transfers are doubtful. This is especially true when one is interested in simulating the effect of hydrophobicity loss in a mixed-wet GDL on the performance of the cell. On the other hand PNM offers a possible approach to analyse fluid transfers in mixed-wet GDL as a function of the fraction of hydrophilic pores. PNM also allows calculating more representative effective transfer coefficients as a function of the fraction of hydrophilic pores.

As sketched in Fig. 1, the general methodology proposed, referred to as the PNM/PM approach, is then to take advantage of both approaches by combining them in the following way: (i) a PNM is used for computing effective transfer coefficients as a function of local properties of GDL, and then (ii) these effective coefficients are used as inputs in PM to compute the performance of the cell.

This three scales methodology allows first coupling between local properties (pore scale) of GDL to its effective properties (Darcy scale), and then to its performance in a PEMFC (macro scale). The loss of hydrophobicity in the GDL is simulated by increasing the fraction  $f$  of hydrophilic pores:  $f=0$  corresponds to a fresh GDL considered as a totally hydrophobic medium of uniform wettability ( $\theta=115^\circ$ );  $0 < f < 1$  corresponds to a partially aged GDL of mixed wettability with a fraction  $f$  of hydrophilic pores ( $\theta=80^\circ$ ) and a fraction  $(1-f)$  of hydrophobic pores ( $\theta=115^\circ$ );  $f=1$  corresponds to a fully aged GDL considered as a totally hydrophilic medium of uniform wettability ( $\theta=80^\circ$ ). As  $f(t)$ , i.e. the evolution of  $f$  as a function of time, is for the time being not

directly measured (see Section 3.3), results are first expressed as a function of  $f$ .

Then the performance is computed as a function of  $t$  under different assumptions on  $f(t)$ . Some of them derive from contact angle measurements available in the open literature (see Section 3).

### 2.2. Thin system through-plane macro-description and PM

PNM allows calculating different fluid transfer coefficients such as liquid and gas permeability, gas diffusion, and capillary pressure as a function of liquid saturation level, e.g. [10] and references therein. Nevertheless, as GDL is a thin system with insufficient scale separation over the thickness, these coefficients are dependent on the size of the volume over which they are calculated (see for instance [18]). In other terms, the concept of local effective coefficient in the through-plane direction becomes meaningless in a thin system (see also [23] for a discussion on the concept of thin porous system). For this reason, in this study we consider coefficients calculated over the complete thickness of the GDL, e.g. [10]. Since these coefficients are not considered as local as in a standard continuum approach to porous media but describes the through-plane behaviour of the entire porous layer, we propose to call them global effective coefficients so as to make a clear distinction with the classical local effective coefficients traditionally associated with the concept of REV (Representative Elementary Volume). The consequence is that the GDL is not meshed across its thickness (OD Model in the thickness). This is an important and original feature of the PNM/PM approach presented in this paper.

The "global effective transfer coefficients" can be seen as transfer functions describing the response of the thin layer as a function of the global saturation level.

In this study, performance of the cell is mainly driven by gas diffusion and not by permeability. So the only global effective transfer coefficient considered is the through-plane gas diffusion coefficient. Note that this coefficient does include the effect of capillarity as it is calculated by the two-phase PNM which takes into account capillary effects (see Section 2.3). In fact, one can distinguish the dry regions in the GDL from the wet ones. The dry regions are the regions where the PM predicts that water is only in the vapour phase. The global effective gas diffusion is constant over time in dry regions. Thus we make the assumption that the possible change in wettability (loss of PTFE) has a negligible impact on the GDL microstructure and therefore on the global effective coefficient. Consequently the global effective diffusion coefficient in dry regions is not subject to degradation and does not vary with time. The wet regions are the regions where the PM predicts that liquid water exists. In wet regions, the global effective diffusion coefficient is calculated at breakthrough that is when liquid water percolates across the GDL. It is a function of  $f$  (and therefore varies with time) but is not a function of the water production. In the quasi-static invasion limit prevailing in PEMFC [18], the liquid distribution inside the GDL for given injection conditions indeed remains the same (and therefore also the gas diffusion) whatever the injected liquid water flux is. We also consider that the loss of

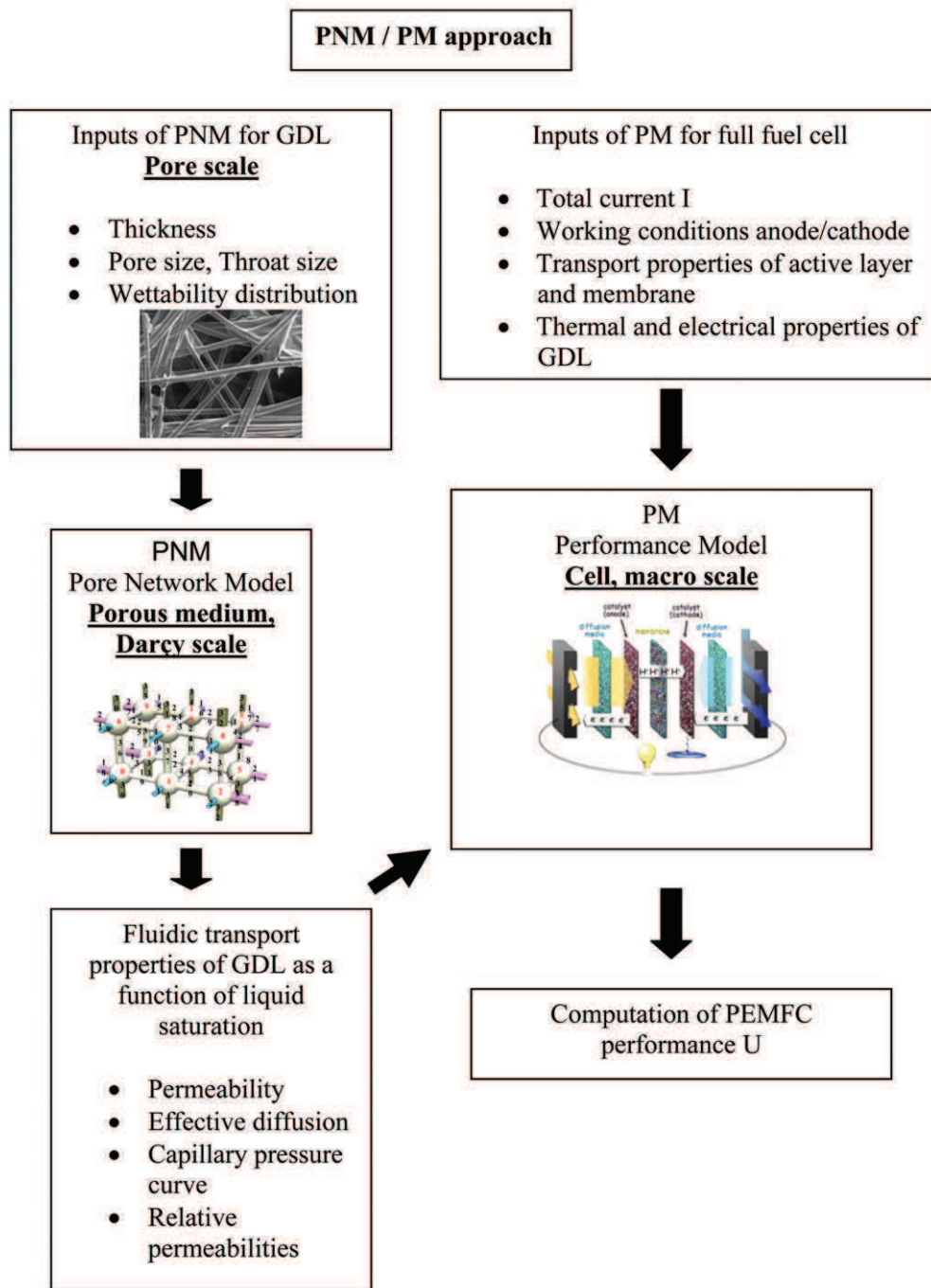


**Fig. 1 – Chart of the PNM/PM approach. In the present study, this approach is applied for increasing wettability of GDL to mimic degradation due to PTFE loss.**

hydrophobicity does not modify the electrical, thermal and mechanical properties of GDL which are then kept constant over time.

Pore network and performance models used in this approach are described in the next two subsections.

### 2.3. Pore network modelling (PNM)

PNM is based on the representation of the pore space in terms of a network of pores (or sites) connected by throats (or

bonds). The “pores” roughly correspond to the larger voids whereas the throats connecting the pores correspond to the constrictions of the pore space. The results useful to the present study were obtained in [10]. For completeness, the main features of PNM used in [10] are briefly summarised in this subsection.

As in many previous works, see [20], and as depicted in Fig. 1, a simple cubic network is considered. Although it would be certainly interesting to use a more realistic representation of GDL pore space skeleton, the simple pore network used in

[10] is *a priori* sufficient to capture the effect of the local changes in wettability properties. It should be also pointed out that models based on more realistic skeletons are in fact not yet available for the fibrous materials forming GDLs. In our case, pores of cubic shape are thus regularly placed on a 3D cartesian grid. Two first neighbour pores are linked by a channel of square cross-section. Such a channel is referred to as a bond or throat. The pore size  $d_p$ , which corresponds to the diameter of the largest sphere inscribed within the pore, is randomly distributed according to a probability law in the range  $[d_{pmin}, d_{pmax}]$ . A Weibull distribution is used in the present study. More precisely, the pore sizes are randomly specified using the expression

$$d_p = d_{pmin} + (d_{pmax} - d_{pmin}) \left[ \{-\delta \ln(\lambda'(1 - \exp(-1/\delta)) + \exp(-1/\delta))\}^{1/\gamma} \right] \quad (1)$$

with  $\delta = 0.1$ ,  $\gamma = 4.7$ ;  $\lambda'$  is random number drawn in the interval  $[0,1]$ . The size  $d_t$  of a throat is then specified as equal to the minimum size of its two adjacent pores,  $d_t = \min(d_{pi}, d_{pj})$ . The results useful to the present study were obtained with  $d_{pmax} = 25 \mu\text{m}$ ,  $d_{pmin} = 10 \mu\text{m}$ , see [10] for more details. These values are representative of pore size distributions in GDL, e.g. [9], and lead to an average porosity of 0.77 for our model GDL.

The network size is characterised by the number of pores placed in each direction. As discussed in [18], a  $40 \times 40 \times 10$  network is considered as representative of a GDL unit cell with the in-plane extension corresponding roughly to the distance between two channels of the bipolar plate. The pore network is fully hydrophobic and hydrophilic when all throats and pores are hydrophobic and hydrophilic, respectively. In a mixed wettability pore network a fraction  $f$  of the pores and of the throat are randomly specified as hydrophilic ( $\theta \sim 80^\circ$ ). The remaining pores and throats are hydrophobic ( $\theta \sim 115^\circ$ ). There are therefore a fraction  $1 - f$  of hydrophobic pores and throats in the network. For convenience, such a network will be referred to as a network containing a fraction  $f$  of hydrophilic “pores” but this means in fact that the fraction of hydrophilic throats and the fraction of hydrophilic pores are both equal to  $f$ .

It is widely admitted that liquid water invasion in a GDL can be computed in the quasi-static limit, that is the invasion is controlled by capillary effects only, [19]. When the porous matrix is sufficiently hydrophobic, quasi-static water invasion can be simulated rather simply using the well-known invasion percolation (IP) algorithm, [24]. When the medium is hydrophilic, the computation is significantly more involved because of cooperative mechanisms controlling the growth of the interface between the two fluids within the pore space, see [10,19] for more details. The PNM results used for the present article were obtained using the quasi-static invasion algorithms described in [10]. Liquid water is injected at the GDL inlet and progressively invades the GDL. The simulation stops at breakthrough that is when the liquid reaches the GDL outlet. The volume fraction of the pore space occupied by liquid water at breakthrough is referred to as the saturation at breakthrough and is denoted by  $S_{BT}$ .

As depicted in Fig. 2, the global saturation at breakthrough as a function of  $f$  computed with the PNM model shows two very distinct behaviours depending of the value

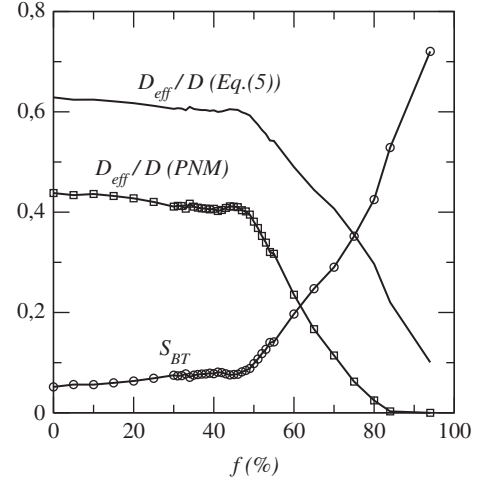


**Fig. 2 – Non-linear effect of loss of hydrophobicity on gas diffusion coefficient through the GDL [10].  $S_{BT}$  is the overall saturation at breakthrough (see text). Eq. (5) in this figure does not refer to an equation in the text but to the classical Bruggeman expression  $D_{eff}(S) = \epsilon^{1.5} (1 - S_{BT})^{1.5} D$  (the figure is imported and adapted from [10]). As can be seen, this classical correlation leads to overestimate the through-plane global effective coefficient compared to the PNM simulations. This coefficient decreases weakly with  $f$  ( $d(D_{eff}/D)/df \approx -0.08$ ) below the percolation threshold ( $f \leq f_c \approx 47\%$ ) whereas the decreasing with  $f$  is quite significant for  $f$  above  $f_c$  ( $d(D_{eff}/D)/df \approx -1.3$ ).**

of  $f$  with respect to the hydrophilic sub-network percolation threshold  $f_c$  ( $f_c \sim 47\%$  here), see again [10] for more details. As can be seen from Fig. 2, the variation of  $S_{BT}$  with  $f$  is quite weak for  $f \leq f_c$ . By contrast,  $S_{BT}$  increases quite significantly with  $f$  when  $f > f_c$ , indicating that the fraction of pore space left free for the gas transport significantly decreases with  $f$  in this range.

The procedure for computing the effective binary diffusion coefficient from pore network simulations is described in several previous GDL related studies, e.g. [9] for example. For a given stage of pore network occupancy by the water, local diffusive conductances are assigned to each pore and throat occupied by the gas phase. Then a linear system of equations is formed by expressing the mass conservation at each gaseous pore of the network and imposing a concentration difference across the network. Solving numerically the linear system gives the concentration of the considered species (i.e. oxygen) at each gaseous pore of network. This allows computing the diffusive flux across the network and then to determine the global effective diffusion coefficient  $D_{eff}$  from the mathematical expression of the through-plane macroscopic flux  $J$ , which is expressed as

$$J = \frac{AD_{eff}}{L} (C_{inlet} - C_{outlet}) \quad (2)$$

where  $A$  is the cross-section area of the porous medium,  $L$  is the porous medium thickness and  $C_{inlet}$  and  $C_{outlet}$  are the concentrations imposed at the inlet and the outlet, respectively. The procedure used in [10] is the same as the one

described in [9] and therefore the details are not given again for the sake of brevity.

The global effective diffusion coefficient was computed as a function of  $f$ , i.e. for the different pore liquid occupancy corresponding to the saturation at breakthrough depicted in Fig. 2. The so obtained evolution of the global effective diffusion coefficient (through-plane coefficient over the whole thickness of the network) is also shown in Fig. 2. Again, one can distinguish two main domains. For  $f$  below  $f_c$ ,  $D_{\text{eff}}$  remains high (of the order of  $0.4-0.5 D$ , where  $D$  is the binary molecular diffusion coefficient) whereas it decreases steadily down to zero (which is reached for  $f \sim 85\%$ ) as  $f$  increases above  $f_c$ .

#### 2.4. Performance modelling (PM)

The PM applies at the cell scale (Fig. 1) with the following assumptions (Fig. 3): the cell operates in co-flux conditions, the membrane/GDL/channels on anode and cathode sides are 1D-meshed (no mesh in the thickness) along the channel length ( $z$  coordinate). This allows focussing on the effect of non-uniform working conditions due to gas composition along the channels, and of liquid water occurrence when the vapour saturation is reached. These non-uniform working conditions are suspected to strongly influence the local current density in the cell and this is the reason why focus is done on this aspect. Active layers are modelled as boundary conditions with semi-empirical laws to compute the electrical potential versus current response as a function of local pressures, temperatures and species concentrations at the active layers interfaces. These local conditions are computed using conservation and mass transport laws in the different

components of the cell (channels, gas diffusion layers, membrane). The main described phenomena are pressure drop in the gas distributors, gas diffusion in the GDL, and liquid water transport in the electrodes, water transport in the membrane, ohmic loss in the membrane, heat production and transfer. The global inputs of the model are the total current, the gases inlet flows and compositions and the cell temperature. The outputs of the model are the cell voltage and the current density distribution. The model gives of course also access to all the local variables, such as the gases compositions inside the cell. The equations of PM are classical and are summarised in the Appendix.

Amongst the different input parameters, the global effective gas diffusion coefficient through the GDL in the presence or not of liquid water is of main interest for the present study. As already described, the GDL is meshed with one cell in the thickness and the global effective gas diffusion coefficients are the ones calculated by PNM (Eq. (2)). For the dry zone (no liquid predicted by the PM), this coefficient corresponds to the intrinsic diffusion coefficient under gas phase conditions (no liquid in the GDL) whereas for the wet zone (existence of liquid water as predicted by the PM) it corresponds to the effective gas diffusion as calculated by PNM (Fig. 2) at breakthrough (liquid water produced by the active layer has reached the interface between GDL and channel).

The gas diffusion layer used (identical on anode and on cathode sides) is the H2315T10A backing from Freudenberg. Its properties have been measured in our laboratory as a function of compression giving values for uncompressed (under the channel) and compressed (under the rib). As the PM used does not differentiate rib and channel, averaged values

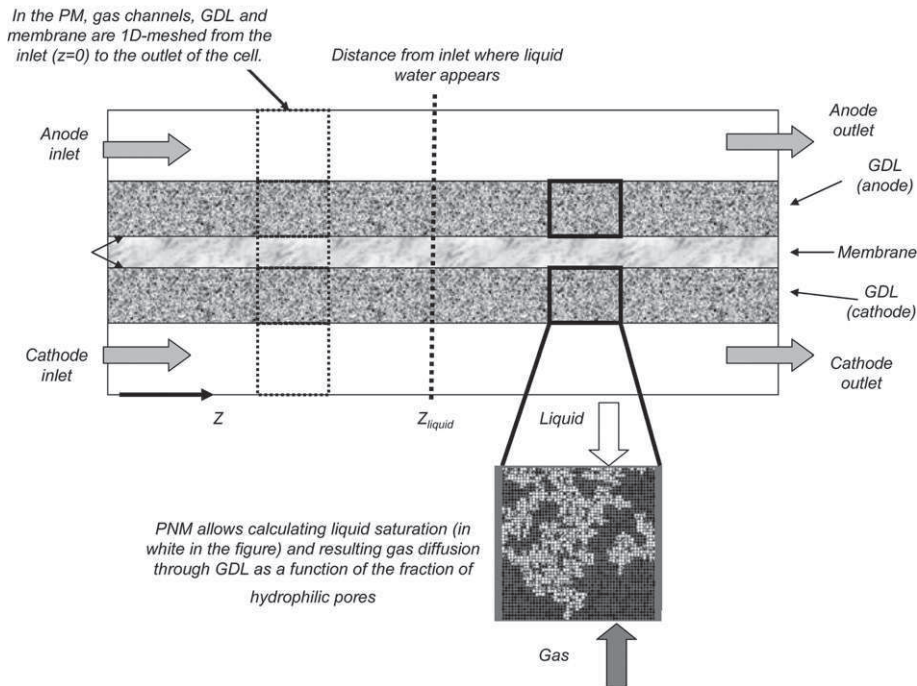


**Fig. 3 – Description of PM and PNM simulation domain. PM is 1D-meshed along the channels and allows calculating the appearance of liquid water. PMN allows calculating effective gas diffusion coefficient through the thickness of the GDL taking into account the existence of liquid water.**

between rib and channel have been used as inputs leading to: thickness 192  $\mu\text{m}$ , thermal conductivity 0.44 W/m/K, porosity 0.77, electrical conductivity 53 S/m.

For a given total current density delivered by the fuel cell, the PM calculates the electrical potential for different gas diffusion coefficient in the GDL, each of them corresponding to different values of  $f$ . The simulation time on an Intel Core 2 Duo (2.66 Ghz) ranges from some minutes (no liquid water and high gas diffusion coefficient) to 1 h (high liquid water content and low gas diffusion coefficient).

## 2.5. The PNM/PM approach

In the PNM/PM coupling approach considered in this article, the GDL is meshed in the PM only along the channels. This is consistent with the fact that scale separation in the GDL is sufficient in the in-plane directions and not in the two others. This 1D-mesh will allow taking into account that liquid saturation and performance are different between the inlet and the outlet of the cell. The two-phase PNM simulations are performed in a 3D domain representative of GDL unit cell (thickness, distance between rib and channel and distance along the channel) to derive effective gas diffusion coefficient taking into account 3D effects in the GDL, especially liquid coalescence which affects largely two-phase pattern and thus gas diffusion and that are completely different between 2D and 3D cases.

The PNM/PM approach is described in Figs. 1 and 3. The approach can be considered as a one way coupling between PM and PNM since the PNM results are input data for the PM. In the present study, this approach is applied for increasing wettability of GDL to mimic degradation due to PTFE loss. This is presented in the next section.

## 3. Degradation of performance due to GDL loss of hydrophobicity

### 3.1. Impact of wettability loss on gas diffusion

As mentioned before, the main idea is to consider that the wettability loss can be represented by the increase in the fraction  $f$  of hydrophilic elements (pores and throats) in the system. As discussed in more detail in [10], this change in wettability has little impact on the water invasion pattern as long as  $f$  is lower than the percolation threshold  $f_c$  of the hydrophilic pore sub-network. The pattern is ramified, see 2D examples in [10], and a significant fraction of the pore space remains free of water, thus available for transport in gas phase. By contrast, the pattern becomes increasingly compact as  $f$  increases in the range  $[f_c, 1]$  and the network becomes almost fully flooded at breakthrough for  $f = 1$ , that is when the network is fully hydrophilic.

Accordingly, as pointed out before and shown in Fig. 2, there is little change in the global saturation at breakthrough  $S_{BT}$  as long as  $f \leq f_c$  whereas the increase in saturation with  $f$  is significant in the range  $[f_c, 1]$ . This in turn induces the evolution of through-plane global diffusion coefficient with  $f$  shown in Fig. 2. The evolution of  $D_{eff}$  is strongly non-linear with two distinct evolutions depending on the value of  $f$  with respect to

the percolation threshold. This coefficient decreases weakly with  $f$  ( $d(D_{eff}/D)/df \approx -0.08$ ) below the percolation threshold whereas the decreasing with  $f$  is quite significant for  $f$  above  $f_c$  ( $d(D_{eff}/D)/df \approx -1.3$ ).

It should be pointed out that the results shown in Fig. 2 were obtained assuming a classical boundary condition at the pore network inlet. As discussed in [25] and in more depth in [23], the water invasion boundary condition to impose at the inlet for the PNM simulations is still somewhat unclear. The classical boundary condition amounts to considering that the GDL is in contact at the inlet with a liquid water reservoir at uniform pressure. However, the GDL backing in an operating fuel cell is in contact with a finer porous layer (the catalyst layer or the microporous layer) and therefore not with a free liquid reservoir. From a purely phenomenological vision of water generation in the catalyst layer, this led to consider in [25] that liquid water enters the GDL rather through a series of independent injection points at the inlet. As shown in [23] and [25], this has a significant impact on pore occupancy at breakthrough compared to the classical free reservoir boundary condition. However, results with this new, probably more realistic, boundary condition for networks of mixed wettability indicate the same tendency as the one shown in Fig. 2, i.e. a significant decrease of  $D_{eff}$  with  $f$  for  $f > f_c$  [26]. For this reason, we have therefore considered, as in most previous works using a PNM approach, see [20], results for  $D_{eff}$  obtained with the traditional boundary condition. This is sufficient to illustrate the capabilities of the PNM/PM approach and to study the impact of wettability loss on performances.

### 3.2. Performance decreases as wettability increases

The above described PM has been applied to simulate the performance of a single-cell (25  $\text{cm}^2$ , co-flux) under the following working conditions:  $\text{H}_2/\text{air}$ , stoichiometry 1.5 (anode) and 1.8 (cathode), gas relative humidity 40% (anode) and 60% (cathode), gas and cell temperature 80  $^\circ\text{C}$ , gas pressure (outlet of the cell) 1.5 bar. Electrical potential is then calculated at 0.6 A/ $\text{cm}^2$ .

In a first step, computations are performed considering a fresh GDL thus simulating the initial conditions ( $t = 0$ ) of the degradation process. As illustrated in Fig. 4, results show that under these working conditions, liquid water forms within the cell on both anode and cathode sides above a certain distance  $z_{\text{liquid}}$  (around 80% of the total length) from the inlet. This is due to the fact that the relative gas humidity in the channel increases along the channel from the inlet to the outlet of the cell inducing an increase of liquid water production. Note here that for fresh and aged GDL liquid water appears on anode and cathode sides at the same position which is due to two main reasons: (i) water transfer through the membrane is very efficient between anode and cathode and (ii) differences between anode and cathode can be smoothed due to the meshing from inlet to outlet. The cell is then shared in two regions: a dry region without liquid water from the inlet up to  $z = z_{\text{liquid}}$ , and a wet region with liquid water from  $z = z_{\text{liquid}}$  up to the outlet. The fact that liquid water is present in the GDL under the initial working conditions (no degradation at  $t = 0$ ) is of course a clear indication that hydrophobicity loss in the GDL is likely to have an impact on performance. One reason is

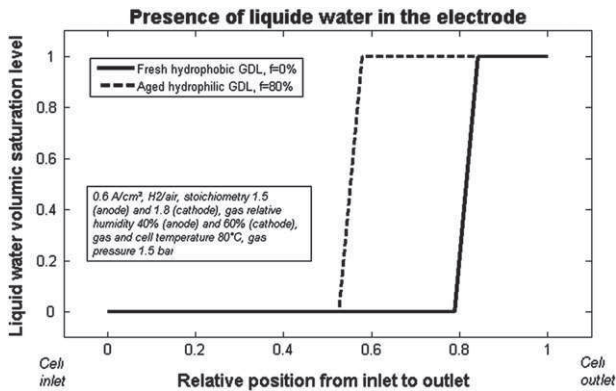


**Fig. 4 – Liquid water appears at the cell outlet and the area of the cell with liquid water is larger with an aged GDL ( $f = 80\%$ ) than with a fresh one ( $f = 0\%$ ).**

that liquid water is supposed to increase hydrophobicity loss and the other reason is that PNM shows that hydrophobicity loss (increase in fraction  $f$  of hydrophilic pores) reduces gas diffusion.

One other output is that the current density is not uniform in the cell. This is shown in Fig. 5. The average value is  $0.6 \text{ A/cm}^2$  (input for the calculation) but local current density decreases from  $0.66 \text{ A/cm}^2$  (at the inlet) to  $0.5 \text{ A/cm}^2$  (at the outlet). As shown in Fig. 6, this is mainly due to the decrease of oxygen fraction due to consumption.

In order to simulate the effect of the wettability increase, the same calculation is then performed for increasing values of fraction  $f$  of hydrophilic pores. It is assumed that  $f$  remains uniform in the whole volume of the GDL, especially between the inlet and the outlet of the cell, which means that we do not consider the influence of liquid water on degradation. This could be added in the future but this dependency remains unknown up-to-date. Nevertheless, a simple sensitivity analysis will be discussed in next section.

For each value of  $f$ , the corresponding value of gas diffusion calculated by PNM is used as an input for the PM. Simulations performed for aged GDL, for example for  $f=0.8$ , show that liquid water progresses up to the inlet (Fig. 4). In the wet region

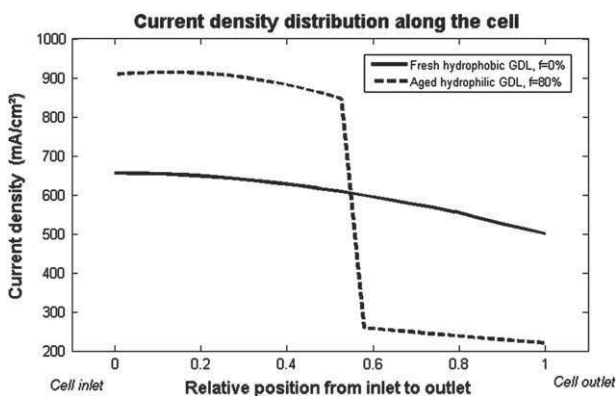


**Fig. 5 – Current density is higher at the cell inlet and non-uniformities of current density are more important with an aged GDL ( $f = 80\%$ ) than with a fresh one ( $f = 0\%$ ).**

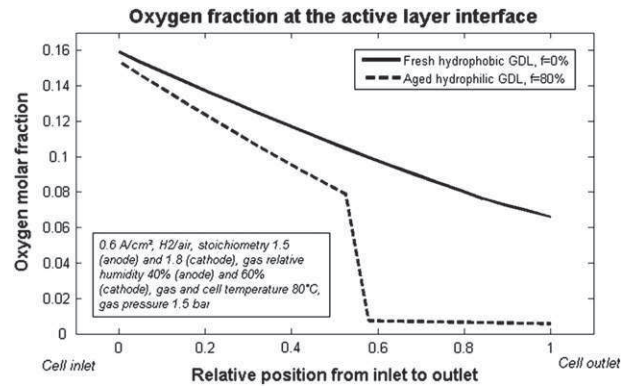


**Fig. 6 – Oxygen fraction at the active layer decreases along the channels and aged GDL ( $f = 80\%$ ) induces a more rapid decrease compared to a fresh one ( $f = 0\%$ ). Note the existence of a flooded area near the outlet with nearly no more oxygen available for electrochemical reaction.**

( $z > z_{\text{liquid}}$ ), wettability and  $f$  will increase, gas diffusion will decrease inducing a reduction of current density. This will be compensated by an increase in current density then in water production in the dry region upstream in which new condensation will then occur at the location where partial vapour pressure is already the highest, i.e. at the interface between dry and wet regions. Degradation will then increase the size of the wet region, which eventually progresses up to cell inlet.

As shown in Fig. 5, this will also increase the current density non-uniformity in the cell, which ranges now between  $0.9 \text{ A/cm}^2$  (at the inlet) and  $0.2 \text{ A/cm}^2$  (at the outlet). This increased non-uniformity is linked to a competition between proton transport due to membrane hydration (improved for the inlet as gas hydration increases) and gas diffusion (reduced towards the outlet as water vapour (and even liquid water) increases and oxygen concentration reduces (Fig. 6)).

These results are summarised in Fig. 7, which also shows that performance decreases as gas diffusion decreases and more rapidly as diffusion approaches roughly 30% of its initial value. Here again we do find a non-linear behaviour of degradation.

It is interesting to point out also that no calculation was possible for  $D_{\text{eff}}(t)/D_{\text{eff}}(t=0) < 0.03$ . This is due to the fact that this low gas diffusion coefficient is obtained for a very low hydrophobicity of the GDL ( $f=0.8$ ) for which the working cell is characterised by larger wet regions occupied by liquid water. In that case the global gas diffusion coefficient (on the whole cell) is not sufficient to maintain the gas flux at the level necessary for the requested current. Under these conditions, the cell can be considered as flooded.

### 3.3. Estimation of degradation rate of performance

The above results clearly show that loss of performance of PEMFC is more than likely when hydrophobicity of GDL decreases due to degradation. The question is now to relate this performance loss with time in order to compare the calculated degradation rate with the experimental one (classically expressed in  $\mu\text{V/h}$ ) and then discuss how far the loss of

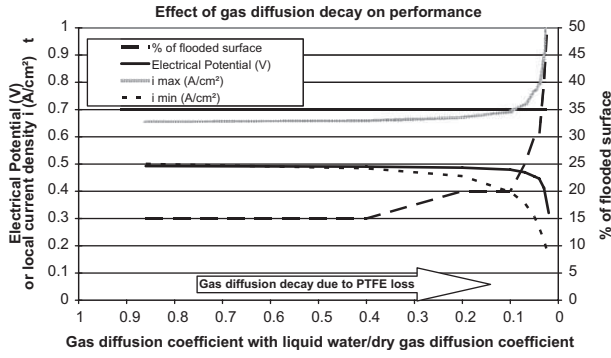


**Fig. 7 – The PTFE loss of the GDL induces liquid water content increase and then gas diffusion decay. This gas diffusion decay leads to a degradation of performance: decrease of electrical potential, increase of flooded surface and increase of current density non-uniformities in the cell.**

hydrophobicity in the GDL is a good candidate to explain the degradation observed in running PEMFC. Notice here that we consider degradation under stationary working conditions and not under transient conditions.

The results presented in previous sections allow calculating the evolution of the electrical potential  $U$  as a function of the hydrophilic pore fraction  $f$  (via the calculation of the gas diffusion inside GDL as a function of  $f$ ). The question is then to assess the value of  $f$  as a function of time in order to compute the evolution of  $U$  with time. Knowing  $f(t)$  the degradation rate of the cell is then simply computed according to

$$\frac{dU}{dt}(t) = \frac{dU}{dD_{\text{eff}}}(D_{\text{eff}}) \times \frac{dD_{\text{eff}}}{df}(f) \times \frac{df}{dt}(t) \quad (3)$$

As previously discussed, wettability of GDL is considered to be mixed. GDL is a porous medium and no real information is available concerning the local wettability and even less concerning its distribution within the volume or its evolution with degradation, so  $f(t)$  remains for the moment unknown. Nevertheless, as presented in Section 1, the measurement of the surface contact angle can be considered up-to-date as reasonable information to assess the loss of hydrophobicity in the GDL. Even if surface contact angle measurements as a function of time are not reported in the literature, some published results [3, fig. 26] show that surface contact angle can be reduced from roughly  $94^\circ$  for fresh GDL down to roughly  $83^\circ$  for GDL after being used 680 h in working PEMFC. These results have been obtained on specific conditions (lifetime tests, Toray Paper TGP-H 090, etc). Therefore they cannot be considered as general. However, they provide a first piece of information to evaluate an order of magnitudes of wettability evolution as a function of time due to GDL degradation. The link between surface contact angle  $\theta^*$  and fraction of hydrophilic pores  $f$  can be roughly evaluated using a Cassie–Baxter formulation such as

$$\cos(\theta^*) = f \times \cos(\theta_{\text{carbone}}) + (1 - f) \times \cos(\theta_{\text{PTFE}}) \quad (4)$$

This formula has been established for flat surface [29] of mixed surface energy and does not include effects such as

surface roughness, non-homogeneities in the volume, etc which are present in a GDL. So here again, even if it is commonly used in the literature for porous media, e.g. [27], it is to be considered as a first rough estimation. This allows calculating the evolution of  $f$  as a function of time

$$f(t) = \frac{\cos(\theta^*(t)) - \cos(\theta_{\text{PTFE}})}{\cos(\theta_{\text{carbone}}) - \cos(\theta_{\text{PTFE}})} \quad (5)$$

Applying this to the measurements from [3, fig. 26] gives  $f(t=0) = 0.59$  (59 % of pores are hydrophilic at the beginning) and  $f(t=680 \text{ h}) = 0.94$  (94% of pores are hydrophilic at the end of the experiment). Assuming then a linear loss of PTFE, the order of magnitude of the degradation rate of the GDL useful in our approach can then be estimated with  $df/dt(t) = 5.2 \times 10^{-4} (\text{h}^{-1})$ . This means that a fully hydrophobic GDL would become fully hydrophilic in 2000 h roughly. As a first step, we also consider that this rate remains constant over time (assuming that degradation of GDL is uniform with time which is to be confirmed even in the case of stationary conditions). Also, no difference is made between anode and cathode (which is questionable as discussed in [5]) or between MPL and backing (which is also questionable as discussed in [6]). Nevertheless, as more detailed information is not available, these assumptions seem reasonable to obtain first tendencies.

Introducing this degradation rate of GDL in relation (3) in combination with  $dU/dD_{\text{eff}}(D_{\text{eff}})$  computed from Performance Model (Fig. 7) and  $dD_{\text{eff}}/df(f)$  computed from Pore Network simulations (Fig. 2), one can evaluate the time dependency of electrical potential  $U$ . This is shown in Fig. 8. As for the influence of  $f$  on  $D_{\text{eff}}$  computed with PNM (Fig. 2), a strong non-linear evolution in the electrical potential  $U$  with time can be seen from Fig. 8, with a significant drop beginning when the fraction  $f$  of hydrophilic pores is around the percolation threshold  $f_c$ . Interestingly, this current potential drop appears much earlier ( $t = 1400 \text{ h}$  roughly) than the time corresponding to a fully hydrophilic GDL (time = 2000 h roughly). Strong non-linear performance drops have already been reported in the literature with different possible explanations such as membrane fracture, catalyst dissolution and poisoning [2],

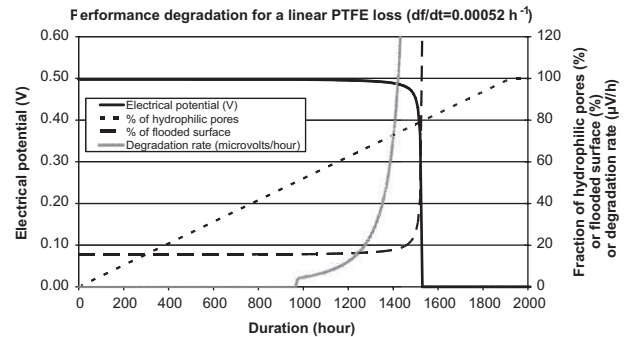


**Fig. 8 – The PTFE loss of the GDL over time induces an increase of fraction of hydrophilic pores and of flooded surface. This leads to a non-linear decrease of electrical potential. In this case PTFE loss is linear and a fully hydrophobic GDL would become fully hydrophilic in 2000 h roughly.**

membrane degradation due to oxidation of bipolar plates [28]. However, the present result shows that strong non-linear performance drop can also appear in relation with loss of hydrophobicity in GDL.

The second output is that the order of magnitude of the time at which this collapse appears is reasonable compared to classical experimental time durations, between 1000 and 20,000 h roughly [2].

The third output is that below the percolation threshold the estimated degradation rate remains rather small (roughly  $-1 \mu\text{V/h}$ ) then increases when  $f$  equals  $f_c$  to reach  $-10$  to  $-20 \mu\text{V/h}$  and even more with increasing  $f$ . These values are of the order of many reported experimental decay rates (around  $2-10 \mu\text{V/h}$ ), i.e. [2] and references therein. More detailed analyses show that even below the percolation threshold the decay rate is not completely constant due to non-linearities in the response of the Performance Model to gas diffusion (mainly due to electrochemical Butler–Volmer relationship). Then near the percolation threshold, non-linearities due to the effect of wettability on gas diffusion are added to the electrochemical non-linearities.

It is important to remind here that fully quantitative comparisons between experiments and these calculations are very difficult for all the previously mentioned reasons: numerous assumptions have been made to compensate for the lack of quantitative knowledge for loss of wettability of GDL; calculations have been performed for stationary conditions and experiments are generally done under cycling conditions (so here we mainly refer to the sometimes called irreversible degradation of performance); hydrophobicity loss is probably dependent on the GDL (as well as to the process used for the hydrophobic treatment) but available data do not even give contact angle measurements for the tests for which performance decay is available; differences should be made between anode, cathode, backing and MPL; diffusion (and percolation threshold) in the GDL is dependent on its structure and is up-to-date simplified in the PNM simulations. Nevertheless it seems reasonable to compare tendencies and orders of magnitude between experiments and our calculations. These first results, although including many assumptions, show that degradation of wettability of GDL is a serious candidate to explain performance loss of PEMFC. This result also shows that loss of hydrophobicity first leads to a decrease of performance due to a decrease in gas diffusion in the wet zones. Then, as  $f$  increases (increase of hydrophilic zones), the wet zone enlarges and this flooding reduces even more the global performance.

Sensitivity analysis on the influence of the GDL degradation rate (as it is one major unknown of this approach) on performance decay rate was performed. Two cases were studied:  $df/dt(t) = 10^{-4}(\text{h}^{-1})$  and  $df/dt(t) = 10^{-3}(\text{h}^{-1})$ . The results are reported in Fig. 9 and show that the time dependency of the cell performance drop (decay rate below percolation threshold and time of performance drop) is, at least to first order, linear with the degradation rate of the GDL. This is mainly due to the fact that up to the percolation threshold, gas diffusion varies, at least to first order, roughly linearly with  $f$ . In the same spirit the influence of a non-constant degradation rate of GDL has been studied to take into account that liquid water is suspected to increase hydrophobicity loss. In this case

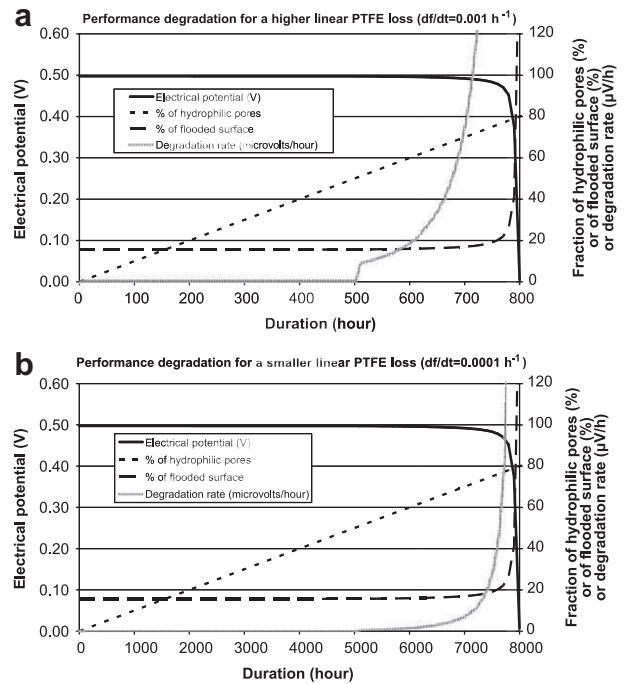


**Fig. 9 – Same case as in Fig. 8 but with higher or smaller loss of PTFE of the GDL. PTFE loss is linear and a fully hydrophobic GDL would become fully hydrophilic in roughly (a) 200 h or (b) 20,000 h. Reduced loss of PTFE would lead to an increased lifetime of the PEMFC.**

we assume a parabolic variation of  $f$  with time with the same total degradation duration compared to the nominal case ( $df/dt = 0.00052$ ). It turns out that the GDL becomes fully hydrophilic in the same time, roughly 2000 h. The results are depicted in Fig. 10 and show that the main modification is linked to the time at which  $f$  reaches  $f_c$  leading to a later appearance of performance collapse. Degradation rate of performance is also modified (reduced in that case) but at a second order.

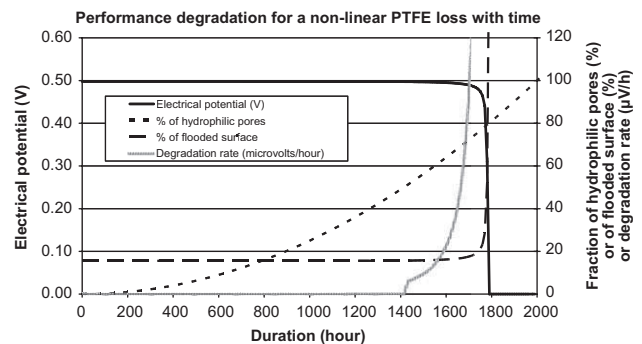


**Fig. 10 – Simulation of performance degradation for a GDL that would become fully hydrophilic in roughly 2000 as in Fig. 8 but with non-linear (increasing with time) degradation compared to a linear one (Fig. 8). In this case, performance degradation is lower than with a linear loss of PTFE.**

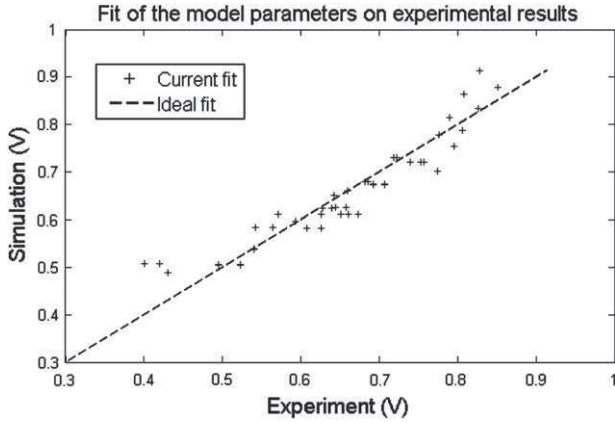


**Fig. 11 – Comparison between experimental (X-axis) and simulated (Y-axis) electrical potential for the different operating conditions used for the fitting of the parameters of the electrochemical law. Ideal fitting would lead to the dashed line (the electrical potential simulated would be always equal to the experimental one) and current fitting is given by (+) for each operating conditions.**

#### 4. Conclusions and perspectives

In this paper we explored the effect of a loss of hydrophobicity of GDL on performance of a PEMFC. In order to link these local changes of wettability at pore scale to macroscopic changes of performance at cell scale, the analysis has been performed using the so-called PNM/PM approach.

The PNM/PM approach is based on a one way coupling between Pore Network Modelling (PNM) and Performance Modelling (PM).

PNM allowed analysing two-phase flows inside GDL of random mixed wettability for which loss of hydrophobicity is simulated by increasing the fraction  $f$  of hydrophilic pores. Results show that gas diffusion decreases as  $f$  increases with a non-linear drop as  $f$  reaches the percolation threshold  $f_c$ .

Then effective gas diffusion coefficient is used as an input of PM to compute electrical performance (potential for a given value of total current) taking into account heat and mass transfer and electrochemical reactions inside a full size 25 cm<sup>2</sup> cell.

Results show that degradation of GDL induces a decrease in electrical potential with a non-linear drop as  $f$  approaches  $f_c$ . The current density distribution is not constant between the inlet and the outlet of the cell. The current density differences in the cell increase with time due to degradation. This is due to the increase of the zone in which liquid water exists. The extent of the wet zone is limited to the cell outlet at the beginning and progresses up to inlet due to hydrophobicity loss. When the fraction of hydrophilic pores  $f$  becomes high enough, flooding occurs and the cell cannot work anymore.

An estimation of degradation rate of GDL was proposed based on the scarce surface contact angle measurements available in the literature. This showed that a fully hydrophobic GDL could become fully hydrophilic in roughly 2000 h. Under this hypothesis, the degradation rate of performance due to degradation of wettability of the GDL could be estimated as roughly  $-1$  to  $-10$   $\mu\text{V/h}$  during the first 1000 h. Then

a sudden collapse of performance occurs. These orders of magnitude are consistent with classical degradation rates observed under various experiments. This suggests that degradation of PTFE in a GDL is a serious candidate to explain, at least in part, the performance degradation of a PEMFC.

This work illustrates also the possibilities offered by coupling or combining PNM and PM in order to link local properties of a component to its performance in a cell. Interesting future work should focus on measuring loss of properties of GDL due to degradation and improve the models to take into account more representative structures, condensation effects and coupling between layers. This approach could also help proposing improvements of structure of GDL to reduce its degradation rate due to PTFE loss.

One can notice also here that the approach presented in this paper could be applied as well to the study of performance loss of DMFC using high concentration methanol [30–32] for which water management is also a critical issue especially on the cathode side. DMFC use very hydrophobic water management layers to provide the water to the anode side. These water management layers are vulnerable to the loss of hydrophobicity as time goes by and this could lead also to performance degradation.

#### Acknowledgements

This work has been performed within the European project DECODE and the Performance Model used has been partly developed and improved in the frame of the French National Project CHAMEAU. The financial support of the European 7th Framework Programme (Grant Agreement 213295), of the French Research Agency (contract ANR-06-PANH-022) and of CEA is gratefully acknowledged.

#### Appendix. Description of the performance model

##### Gas distributors

Anode and cathode gas channels are 1D-meshed (Fig. 3) from the gas inlets to the gas outlets.

Mass and thermal balances are computed on each cell of the mesh considering gas inlet, gas outlet, oxygen or hydrogen consumption, water production, water condensation or evaporation and heat exchanges with the bipolar plate and the gas diffusion layer. Pressure drop is modelled using simplified linear correlations [33].

$$Q = \frac{\nabla P}{K_p} \quad (\text{A-1})$$

$Q$  is the volumic flow rate and  $K_p$  the pressure drop coefficient.

##### Gas diffusion layers

The anode and cathode GDL are 1D-meshed from the gas inlets to the gas outlets.

The diffusion fluxes in the gas phase are driven by the inverted Stefan–Maxwell equations [34]. The molar fluxes  $N_i$  are computed from the molar fraction gradient, the molar masses  $M_i$  of the species, the gas concentration  $c_g$  and the gas density  $\rho_g$ .

$$N_x = \frac{c_g^2}{\rho_g} \cdot (M_v \cdot D_{xv}^T \cdot \nabla X_v + M_n \cdot D_{xn}^T \cdot \nabla X_n) \quad (\text{A-2})$$

$$N_n = \frac{c_g^2}{\rho_g} \cdot (M_v \cdot D_{nv}^T \cdot \nabla X_v + M_x \cdot D_{nx}^T \cdot \nabla X_x) \quad (\text{A-3})$$

$$N_v = \frac{c_g^2}{\rho_g} \cdot (M_n \cdot D_{vn}^T \cdot \nabla X_n + M_x \cdot D_{vx}^T \cdot \nabla X_x) \quad (\text{A-4})$$

The diffusion coefficients  $D_{ij}^T$  in a ternary (3 species) mixture used in these equations are deduced from the binary diffusion coefficients  $D_{ij}$ , considering the molar fraction  $x_i$  and the molar mass  $M_i$  of each species.

$$D_{ij}^T = D_{ij} \left[ 1 + \frac{X_k \left( \frac{M_k}{M_j} D_{ik} - D_{ij} \right)}{X_i D_{jk} + X_j D_{ik} + X_k D_{ij}} \right] \quad (\text{A-5})$$

The values of the binary diffusion coefficient in the presence or not of liquid water are directly given by the pore network model: in the absence of liquid water the diffusion coefficient is the value computed for diffusion through the dry porous media and in the presence of liquid water it is deduced from Fig. 2 depending on the fraction  $f$  of hydrophilic pores. These relations are used both on the anode and on the cathode sides.

Vapour fraction is compared to vapour saturation to determine the presence or not of liquid water.

$$X_{\text{sat}} = \frac{P_{\text{sat}}(T)}{P} \quad (\text{A-6})$$

## Membrane

The membrane is 1D-meshed from the gas inlets to the gas outlets.

The water content of the electrolyte is computed dynamically from the interfacial conditions. Equilibriums with hydration conditions in the electrodes are given for anode and cathode side by [35]:

$$\lambda = \begin{cases} \text{if } a \leq 1 \text{ then } & 0.043 + 17.81 \cdot a - 39.85 \cdot a^2 + 36.0 \cdot a^3 \\ \text{else } & 14 + 1.4 \cdot (a - 1) \end{cases} \quad (\text{A-7})$$

where  $a$  is the water activity in the electrode at the interface with the membrane and  $\lambda$  is the water content of the membrane at the interface with the electrode. The diffusion coefficient is estimated using [35]:

$$D_\lambda = (6.707 \times 10^{-8} \cdot \lambda + 6.387 \times 10^{-7}) \cdot \exp\left(-\frac{2416}{T}\right) \quad (\text{A-8})$$

and the diffusion flux through the mesh cell is computed using [36]

$$N_{\text{diff}} = \frac{\rho_{\text{dry}}}{EW} \cdot D_\lambda \cdot \nabla \lambda \quad (\text{A-9})$$

where  $N_{\text{diff}}$  is the flux of diffusion ( $\text{mol m}^{-2} \text{s}^{-1}$ ),  $\rho_{\text{dry}}$  is the density of the dry Nafion and  $EW$  is the equivalent weight of

the Nafion [36]. In the same way, the electro-osmosis flux is given by [37]

$$N_{\text{eo}} = \frac{n_{\text{eo}} \cdot I}{2F} \quad (\text{A-10})$$

where  $N_{\text{eo}}$  is the electro-osmotic drag molar flux,  $I$  is the current density,  $n_{\text{eo}}$  is the electro-osmotic drag coefficient, and  $F$  is the Faraday constant.

According to ref. [37]

$$n_{\text{eo}} = 1.0 + 0.028 \cdot \lambda + 0.0026 \cdot \lambda^2 \quad (\text{A-11})$$

## Active layers

Active layers are considered as thin interface linking membrane and GDL.

The electrochemical response of the model is based on a semi-empirical model, as proposed by Amphlett [38,39]

Global cell potential (for one cell) is given by

$$U = E_{\text{rev}} + \eta_{\text{act}} - R_m \cdot I \quad (\text{A-12})$$

where

$$E_{\text{rev}} = \alpha_1 + \alpha_2 \cdot (T - 298.15) + \alpha_3 \cdot T \cdot (0.5 \cdot \ln P_{\text{O}_2} + \ln P_{\text{H}_2}) \quad (\text{A-13})$$

is the thermodynamic potential and

$$\eta_{\text{act}} = \beta_1 + \beta_2 \cdot T + \beta_3 \cdot T \cdot \ln I + \beta_4 \cdot T \cdot \ln P_{\text{O}_2} + \beta_5 \cdot T \cdot \ln P_{\text{H}_2} \quad (\text{A-14})$$

is the activation over-voltage. The temperature  $T$  and the partial pressures  $P_{\text{O}_2}$ ,  $P_{\text{H}_2}$  are the local conditions at the active layers of the electrodes. The coefficient  $\alpha_i$  is calculated from thermodynamical parameters (reactions enthalpy and entropy changes).  $R_m$  is the membrane electrical resistivity.

$$R_m = \frac{e_m}{\sigma} \quad (\text{A-15})$$

with [40]

$$\sigma = (33.75 \cdot \lambda - 21.41) \cdot \exp\left(-\frac{1268}{T}\right) \quad (\text{A-16})$$

The coefficient  $\beta$  has been fitted to experimental results. For this, performance tests have been performed in-house on a single-cell for different operating conditions of pressure (1.5 bar), temperature (50 °C and 80 °C), hydration level (60% and 80% on anode and on cathode sides, respectively) and reactant fraction (from 4% to 100% O<sub>2</sub>, 100% H<sub>2</sub>) [41]. A fitting procedure has then been applied to define the set of  $\beta$  parameters that would allow simulating these experimental conditions best. Comparisons between measured and simulated cell electrical potentials for each operating conditions are given in Fig. 11.

The values of the parameters deduced from this fitting and used in the PM are:

$$\begin{cases} \alpha_1 = 1.4824 \\ \alpha_2 = -1.593 \times 10^{-3} \\ \alpha_3 = 4.3085 \times 10^{-5} \end{cases}$$

$$\begin{cases} \beta_1 = -1.2717 \\ \beta_2 = 0.0028799 \\ \beta_3 = -0.0002831 \\ \beta_4 = 0.00020313 \\ \beta_5 = 0 \end{cases}$$

## REFERENCES

---

- [1] Wang Y, Chen K, Mishler J, Cho SC, Adroher XC. *Appl Energy*; 2010;981–1007.
- [2] Wu J, Yuan X, Martin J, Wang H, Zhang J, Shen J, et al. *J Power Sources* 2008;184:104–19.
- [3] Borup R, Meyeres J, Pivovar B, Kim Y, Mukundan R, Garland N, et al. *Chem Rev* 2007;107:3904–51.
- [4] Williams M, Begg E, Bonville L, Kunz R, Fenton J. *J Electrochem Soc* 2004;151(8):A1173–80.
- [5] Schulze M, Wagner N, Kaz T, Friedrich A. *Electrochim Acta* 2007;52:2328–36.
- [6] Tian Y, Sun G, Mao Q, Wang S, Liu H, Xin Q. *J Power Sources* 2008;185:1015–21.
- [7] Wu J, Martin J, Orfino F, Wang H, Legzdins C, Yuan X, et al. *J Power Sources* 2010;195:1888–94.
- [8] Sinha PK, Wang CY. *Chem Eng Sci* 2008;63:1081–91.
- [9] Gostick J, Ioannidis M, Fowler M, Pritzker M. *J Power Sources* 2007;173:277–90.
- [10] Pulloor Kuttanikkad S, Prat M, Pauchet J. *J Power Sources* 2011;196:1145–55.
- [11] Mazumder S, Cole J. *J Electrochem Soc* 2003;150(11):A1510–7.
- [12] Weber A, Darling R, Newman J. *J Electrochem Soc* 2004;151(10):A1715–27.
- [13] You L, Liu H. *J Power Sources* 2006;155:219–30.
- [14] Shah A, Kim G, Sui P, Harvey D. *J Power Sources* 2007;163:793–806.
- [15] Becker J, Wieser C, Fell S, Steiner K. *J Electrochem Soc* 2009;156(10):B1175–81.
- [16] Gostick J, Fowler M, Pritzker M, Ioannidis M, Behra J. *J Power Sources* 2006;162:228–38.
- [17] Gurau V, Bluemle M, De Castro E, Tsou Y, Zawodzinski T, Mann J. *J Power Sources* 2007;165:793–802.
- [18] Rebai M, Prat M. *J Power Sources* 2009;192:534–43.
- [19] Chapuis O, Prat M, Quintard M, Chane-Kane E, Guillot O, Mayer N. *J Power Sources* 2008;178:258–68.
- [20] Mukherjee PP, Kang Q, Wang C. *Energy Environ Sci* 2011;4:346–69.
- [21] Mukherjee P, Mukundan R, Borup R. Proceedings of the ASME 2010 eighth international fuel cell science, engineering and technology conference, Brooklyn, USA; 2010.
- [22] Seidenberger K, Wilhelm F, Schmitt T, Lehnert W, Scholta J. *J Power Sources* 2011;196(2):5317–24.
- [23] Ceballos L, Prat M, Duru P. *Physical Review E*; in press.
- [24] Wilkinson D, Willemsen JF. *J Phys A Math Gen* 1983;16:3365–76.
- [25] Ceballos L, Prat M. *J Power Sources* 2010;195:825–8.
- [26] Ceballos L. Ph.D thesis, INPT; 2011.
- [27] Ustohal P, Stauffer F, Dracos T. *J Contam Hydrol* 1998;33:5–37.
- [28] Wind J, Späh R, Kaiser W, Böhm G. *J Power Sources* 2002;105:256–60.
- [29] Cassie ABD, Baxter S. *Trans Faraday Soc* 1944;40:546–51.
- [30] Bahrami H, Faghri A. *J Fuel Cell Sci Technol* 2011;8(1–15):021011.
- [31] E Shaffer C, Wang CY. *Electrochim Acta* 2009;54(24):5761–9.
- [32] Bahrami H, Faghri A. *J Electrochem Soc* 2010;157(12):B1762–76.
- [33] Dauphin-Tanguy G. *Les Bonds Graphs*. Hermes; 2000.
- [34] Bird RB, Stewart WE, Lightfoot EN. *Transport phenomena*. Wiley International; 1960.
- [35] Zawodzinski TA, Davey J, Valerio J, Gottesfeld S. *Electrochim Acta* 1995;40(3):297–302.
- [36] Gerbaux L. Ph.D thesis, INPG; 1996.
- [37] Meier F, Eigenberger G. *Electrochim Acta* 2004;49(11):1731–42.
- [38] Amphlett JC, Baumert RM, Mann RF, Peppley BA, Roberge PR, Harris TJ. *J Electrochem Soc* 1995;142(1):1–8.
- [39] Amphlett JC, Baumert RM, Mann RF, Peppley BA, Roberge PR, Harris TJ. *J Electrochem Soc* 1995;142(1):9–15.
- [40] Springer TE, Zawodzinski TA, Gottesfeld S. *J Electrochem Soc* 1991;138(8):2334–42.
- [41] Poirot-Crouvezier JP. Ph.D thesis, INPG; 2000.